25. R. Brett, *Geochim. Cosmochim. Acta* **48**, 1183 (1984).
26. I. Y. Azbel, I. N. Tolstikhin, J. D. Kramers, G. Pechernikova, A. V. Vityazev, *ibid.* **57**, 2889 (1993).
27. S. R. Jurewicz and A. J. G. Jurewicz, *J. Geophys. Res.* **91**, 9277 (1986).
28. W. F. Brace and J. B. Walsh, *Am. Mineral.* **47**, 1111 (1962); H. S. Waff and U. H. Faul, *J. Geophys. Res.* **97**, 9003 (1992).
29. We thank M. Hirschmann for discussions that motivated the initial experiments, and G. Gwanmesia, B. Li, and R. Lieberman, who helped with preliminary multianvil work. Reviews by J. Brenan, D. Farber, and N. Marchildon improved the manuscript. Supported by the Lawrence Livermore National Laboratory Institute of Geophysics and Planetary Physics (F.J.R.) under the auspices of Department of Energy contract W-7405-Eng-48. Additional support was provided by National Science Foundation grants EAR-8717341 and EAR-9105055 to E.B.W.

7 December 1995; accepted 12 March 1996

Role of Type I Myosins in Receptor-Mediated Endocytosis in Yeast

M. Isabel Geli and Howard Riezman*

Type I myosins are thought to drive actin-dependent membrane motility, but the direct demonstration in vivo of their involvement in specific cellular processes has been difficult. Deletion of the genes *MYO3* and *MYO5*, which encode the yeast type I myosins, almost abolished growth. A double-deleted mutant complemented with a *MYO5* temperature-sensitive allele (*myo5-1*) showed a strong defect in the internalization step of receptor-mediated endocytosis, whereas the secretory pathway remained apparently unaffected. Thus, myosin I activity is required for a budding event in endocytosis but not for several other aspects of membrane traffic.

Type I myosins constitute a large family of ubiquitous actin- and adenosine triphosphate (ATP)–dependent molecular motors with a distinct COOH-terminal tail domain. Instead of the coiled-coil region that allows dimerization of conventional myosins, type I myosins possess a short positively charged tail that in many cases binds acidic phospholipids (*1*). Their biochemical characteristics and subcellular localization to intracellular membranes suggest an involvement in actin-dependent membrane motility processes such as organelle movement, vesicle trafficking, phagocytosis, pinocytosis, membrane ruffling, or lamellipodia formation (*2*). However, direct demonstration of their requirement in vivo for these functions has been difficult because of their functional redundancy and the lack of established quantitative functional assays (*1*).

Only one type I myosin has been described in the yeast *Saccharomyces cerevisiae*: Myo3p. Deletion of the *MYO3* gene does not lead to any phenotypic change, which suggests functional redundancy (*3*). We have used a polymerase chain reaction (PCR) screening approach (*4*) to isolate a second gene, *MYO5*, that encodes a type I myosin with 87% amino acid sequence identity to Myo3p (Fig. 1A). The head and tail domains are separated by three IQ (isoleucine-glutamine) motifs, which would be predicted to bind calmodulin, a key regulator of myosin I activity (*2*). A second level of regulation is specifically provided in type I myosins by a phosphorylation site placed between the ATP and the actin binding sites [S357 (Ser^{357})] (*5*). Phosphorylation in vitro of the ameboid type I myosins causes a 20-fold activation of the adenosine triphosphatase activity (*5*). The tail of Myo5p contains two distinct features that are shared with other yeast and ameboid type I myosins: a proline-rich region that may constitute a second ATP-independent actin binding site, and an SH3 (Src homology 3) domain proposed to mediate protein-protein interaction (*2*). Recently, two SH3-containing type I myosins have been isolated from mammalian cells (*6*). The yeast Myo5p and Myo3p show maximal homology to *Acanthamoeba* myosin IB (AMIB) and *Dictyostelium* myosin IB (*7*). Both myosins localize to the plasma membrane. The phosphorylated form of AMIB concentrates to actively motile regions of the plasma membrane (*7*). Double-deletion mutants in *Dictyostelium* type I myosins (*myoA*/*myoB*$^-$ or *myoC*/*myoB*$^-$) show conditional defects in fluid-phase pinocytosis (*7*). Deletion of *MYO5*, as with deletion of *MYO3* (*3*), did not lead to any observable alterations in growth properties (*8*). However, combination of both deletions in the same haploid resulted in a severe growth defect (*9*).

One of the main processes that requires plasma membrane deformation in nonmitotic yeast is the internalization step of endocytosis. Actin and calmodulin, two key proteins associated with myosin function, are required in this process (*10*). Thus, it is possible that a type I myosin could play a role in the uptake step of receptor-mediated endocytosis.

Endocytic internalization can be monitored by measurement of the percentage of ^{35}S-labeled α-factor bound to its receptor (Ste2p), which becomes resistant to an acid wash (pH 1) over time (*11*). We used this assay to measure the efficiency of receptor-mediated internalization in *myo3*Δ and *myo5*Δ mutant strains (*9*) (Fig. 1, B and C). The *myo3*Δ strain showed wild-type (WT) internalization kinetics. In contrast, we detected a strong internalization defect in the

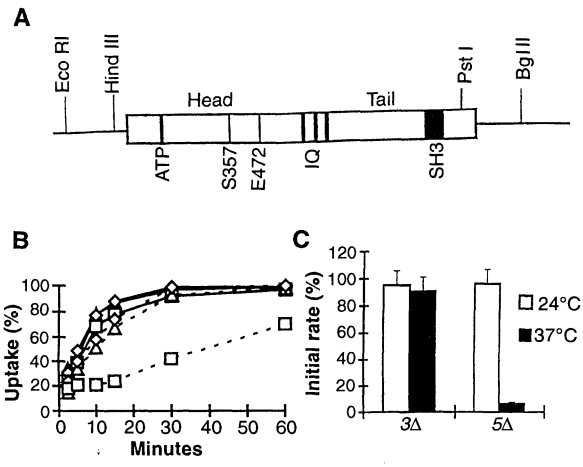

Fig. 1. *myo5*Δ but not *myo3*Δ is defective for α-factor internalization. (**A**) Structure of *MYO5* (GenBank/EMBL/DDBJ accession number SC9718; open reading frame 15772 to 19429). IQ, IQ motifs; ATP, ATP binding site; S357, putative phosphorylation site; SH3, SH3 domain. (**B**) RH3376 (WT, triangles), RH3377 (*myo3*Δ, diamonds), and RH3378 (*myo5*Δ, squares) (*9*) were assayed at 24°C (solid lines) or 37°C (dashed lines) as described (*11*). Cells were grown to logarithmic phase in synthetic dextrose yeast extract (SDYE) at 24°C. Biosynthetically labeled ^{35}S–α-factor was bound for 45 min on ice in yeast extract, peptone, uracil, adenine, and dextrose (YPUAD) medium. Cells were centrifuged and resuspended in YPUAD medium at 24°C or 37°C. Samples were taken at the indicated time points into pH 1 and pH 6 buffer to monitor internalized versus total cell-associated radioactivity. The results are expressed as the percentage of total counts internalized. The values correspond to the average of at least two independent experiments, with standard deviations smaller than 10% (20% at the initial time point). (**C**) The initial uptake rates (internalized counts per minute) were calculated for each experiment in the linear range. The average value of each mutant strain was divided by the corresponding WT values at the appropriate temperature and expressed as a percentage.

Department of Biochemistry, Biozentrum, University of Basel, Klingelbergstrasse 70, Basel, CH-4056, Switzerland.

*To whom correspondence should be addressed.

myo5Δ strain at 37°C but not at 24°C. Thus, it was likely that Myo3p could replace Myo5p function in endocytosis at 24°C but not at 37°C.

To test this hypothesis, we constructed a temperature-sensitive (ts) allele of *MYO5* (*myo5-1*) by analogy to the *myo2-66* allele [E511K ($Glu^{511} \rightarrow Lys^{511}$)] of the essential yeast myosin V *MYO2* (*12*). The strain in which *myo5-1* replaced *MYO5* (*13*) showed α-factor uptake kinetics similar to those of the *myo5Δ* strain at 24°C and 37°C (Fig. 2A), but the initial uptake rate at 37°C was not as severely affected (Figs. 1C and 2C). Thus, the *myo5-1* allele was strongly defective at 37°C, although it retained some residual activity at this temperature.

The pmyo5-1 plasmid was able to rescue the *myo3Δ myo5Δ* mutant for its growth phenotype at 24°C, but growth was strongly reduced at 37°C (*13*). The time courses of internalization by *myo3Δ myo5Δ* strains carrying WT or ts forms of Myo5p are shown (Fig. 2B). The initial uptake rate at 24°C in strains expressing ts Myo5p was only 48% of that in the control strain (Fig. 2C). A partial lack of function at 24°C is also found for the *myo2-66* allele (*12*). Comparison between the uptake rates of strains expressing ts Myo5p in the presence or absence of Myo3p at 24°C (Fig. 2C, 5Δ versus 3Δ5Δ) showed that Myo3p can substitute for Myo5p at this temperature. Because shift of the *myo3Δ myo5Δ* pmyo5-1 strain to 37°C caused an immediate decrease in the initial uptake rate to 6% of that of the control strain (Fig. 2C), it is likely that Myo5p plays a direct role in the uptake step of endocytosis.

We also monitored internalization of the α-factor receptor (Ste2p) directly by immunofluorescence (*14*) (Fig. 2D). Ste2p disappeared from the surface of cells expressing WT Myo5p within 15 min after addition of α-factor at 37°C. The protein then concentrated in a bright spot near the vacuole, which corresponds to late endosomes (*14*). In contrast, Ste2p remained at the cell surface in cells expressing only the ts Myo5p, which confirmed the defect in receptor-mediated endocytosis demonstrated above.

MYOA from *Aspergillus* shows similarity to Myo3p and Myo5p (*15*), and its depletion results in enlarged cells that are incapable of hyphal extension and have reduced levels of extracellular acid phosphatase activity. Together with the immunolocalization of the myosin at the hyphal tip, this led to the proposal that *MYOA* is involved in the transport of components to sites of growth (*15*). To test whether Myo3p and Myo5p function in the secretory pathway, we assayed cells expressing only the ts Myo5p for invertase secretion (*10*) (Fig. 3A). Maturation and secretion of invertase were normal at 37°C. Biosynthetic traffic to the vacuole was also unaffected, as monitored by pulse-chase analysis of carboxypeptidase Y (*16*) (Fig. 3B). Thus, type I myosins are required for a specific process in yeast membrane traffic: the uptake step of receptor-mediated endocytosis.

The fact that the *myo3Δ myo5Δ* double mutant grew extremely poorly at 24°C suggests that these molecules are required for processes other than endocytosis (*17*). The *myo3Δ myo5Δ* pmyo5-1 strain showed a disorganized actin cytoskeleton at 24°C (*8*). It is likely that type I myosins are also involved in the organization of the cortical actin cytoskeleton in yeast (*18*). A disrupted actin cytoskeleton is found in other endocytosis mutants (*19*). The defect we observed in endocytosis was not solely due to the disruption of the actin cytoskeleton, as some mutants with disorganized actin have no defect in receptor-mediated endocytosis (*20*).

Actin-dependent endocytic pathways

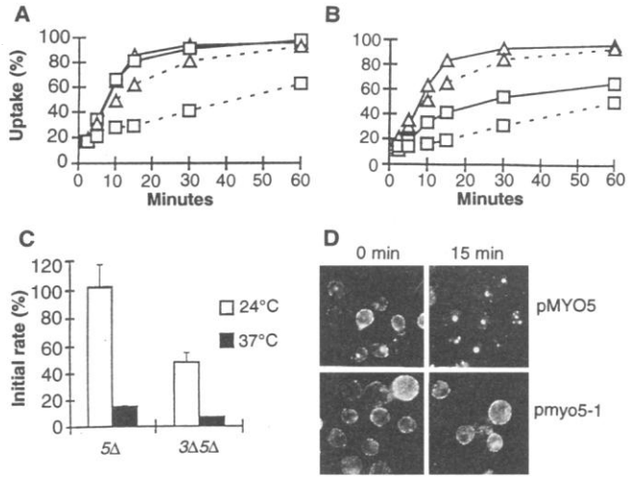

Fig. 2. Myo5p is required for α-factor receptor internalization. (**A**) Internalization assays on RH3380 (*myo5Δ* pmyo5-1, squares) and RH3382 (*myo5Δ* pMYO5, triangles) (*13*) (see legend of Fig. 1) at 24°C (solid lines) and 37°C (dashed lines). (**B**) Internalization assays on RH3383 (*myo3Δ myo5Δ* pmyo5-1, squares) and RH3384 (*myo3Δ myo5Δ* pMYO5, triangles) at 24°C (solid lines) and 37°C (dashed lines) (*13*). (**C**) Initial uptake rates of RH3380 and RH3383 strains expressed as percentages of the RH3382 and RH3384 values, respectively. (**D**) Ste2p endocytosis by RH3384 and RH3383. The experiment was performed as described (*14*). The strains were grown to logarithmic phase on SDYE medium at 24°C. Cells were incubated for 10 min at 37°C in the presence of cycloheximide. α-Factor was added and samples were taken and processed for immunofluorescence at the indicated time points. A polyclonal antibody raised against Ste2p (*22*) was used.

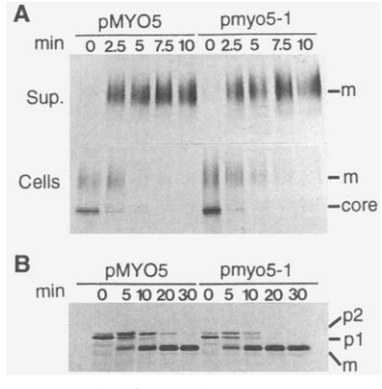

Fig. 3. Type I myosins are not required for invertase secretion and carboxypeptidase (CPY) maturation. (**A**) Invertase secretion. Pulse-chase labeling of invertase was performed as described (*10*). RH3384 (pMYO5) and RH3383 (pmyo5-1) were grown to logarithmic phase on SDYE at 24°C, converted to spheroplasts, and incubated in low glucose medium to induce invertase expression. Cells were centrifuged and resuspended in 37°C prewarmed medium. After 5 min of incubation, cells were pulsed for 4 min with ^{35}S-methionine and ^{35}S-cysteine and chased for the indicated times. Spheroplasts were separated from the medium to assay internal (Cells) and external (Sup.) invertase by immunoprecipitation, gel electrophoresis, and fluorography; core, core glycosylated form; m, hyperglycosylated form. (**B**) CPY maturation. CPY pulse-chase labeling was performed as described (*16*). Cells were grown to logarithmic phase in SDYE medium at 24°C, centrifuged, resuspended in prewarmed medium (37°C), and pulse-labeled as described above. Cells were chased until the indicated times and analyzed as for invertase; p1, endoplasmic reticulum form; p2, Golgi form; m, mature vacuolar form.

Table 1. *Saccharomyces cerevisiae* strains used in the experiments. All strains were *MATa his3 leu2 trp1 ura3 bar1*.

Strain name	Genotype
RH3376	*MYO3 MYO5*
RH3377	*myo3Δ::HIS3 MYO5 ade2*
RH3378	*MYO3 myo5Δ::TRP1 ade2*
RH3382	*MYO3 myo5Δ::TRP1* pMYO5::*URA3 ade2*
RH3380	*MYO3 myo5Δ::TRP1* pmyo5-1::*URA3 lys2 ade2*
RH3384	*myo3Δ::HIS3 myo5Δ::TRP1* pMYO5::*URA3 lys2*
RH3383	*myo3Δ::HIS3 myo5Δ::TRP1* pmyo5-1::*URA3 lys2*

have been described in many cell types (*21*). It is likely that type I myosins play an important role in endocytic internalization via these pathways.

REFERENCES AND NOTES

1. T. Hasson and M. S. Mooseker, *Curr. Opin. Cell Biol.* **7**, 587 (1995).
2. R. E. Cheney and M. S. Mooseker, *ibid.* **4**, 27 (1992); J. A. Hammer, *J. Muscle Res. Cell. Motil.* **15**, 1 (1994).
3. H. V. Goodson and J. A. Spudich, *Cell Motil. Cytoskeleton* **30**, 73 (1995).
4. W. M. Bement, T. Hasson, J. A. Wirth, R. E. Cheney, M. S. Mooseker, *Proc. Natl. Acad. Sci. U.S.A.* **91**, 6549 (1994).
5. J. L. Tan, S. Ravid, J. A. Spudich, *Annu. Rev. Biochem.* **61**, 721 (1992).
6. W. M. Bement, J. A. Wirth, M. A. Mooseker, *J. Mol. Biol.* **243**, 356 (1994); H. E. Stöffler, C. Ruppert, J. Reinhard, M. Bähler, *J. Cell Biol.* **129**, 819 (1995).
7. I. C. Baines, A. Corigliano-Murphy, E. D. Korn, *J. Cell. Biol.* **130**, 591 (1995). K. D. Novak, M. D. Peterson, M. C. Reedy, M. A. Titus, *ibid.* **131**, 1205 (1995).
8. M. I. Geli and H. Riezman, data not shown.
9. *MYO3* and *MYO5* were deleted in the same diploid to obtain a heterozygotic strain, RH3375 (*MATa/MATα ade2/ADE2 his3/his3 myo3Δ::HIS3/MYO3 myo5Δ::TRP1/MYO5 leu2/leu2 lys2/LYS2 trp1/trp1 ura3/ura3 bar1/bar1*). From this strain the RH3376, RH3377, and RH3378 strains were generated by tetrad dissection (Table 1). Deletion of *MYO3* has been described (*6*). For deletion of *MYO5*, the fragments Eco RI–Hind III and Pst I–Bgl II (Fig. 1A) were used to flank a 0.9-kb DNA fragment carrying the *TRP1* gene. The spores were analyzed by replica plating on synthetic dextrose medium lacking the corresponding amino acids. None of the predicted double mutants (*TRP1 HIS3*) out of 20 dissected tetrads formed colonies. A double mutant harboring plasmid pmyo5-1 or pMYO5 (*13*) was able to form pinpoint-sized colonies upon plasmid loss. When the pmyo5-1–carrying strain was shifted to 37°C, the proportion of unbudded cells did not change.
10. E. Kübler and H. Riezman, *EMBO J.* **12**, 2855 (1993); E. Kübler, F. Schimmöller, H. Riezman, *ibid.* **13**, 5539 (1994).
11. V. Dulić *et al.*, *Methods Enzymol.* **194**, 697 (1991).
12. E511 (Glu511) of Myo2p in the putative actin binding domain [G. C. Johnston, J. A. Pendergast, R. A. Singer, *J. Cell Biol.* **113**, 539 (1991)] corresponds to E472 (Glu472) in Myo5p (Fig. 1A). The allele E472K (Glu472 → Lys472) (*myo5-1*) was generated by PCR and cloned into a centromere-based plasmid [YCplac33; *Gene* **74**, 527 (1988)] to generate pmyo5-1. Wild-type *MYO5* was also cloned into YCplac33 to generate pMYO5.
13. RH3380, RH3383, RH3382, and RH3384 strains (Table 1) were generated by tetrad dissection from RH3375 (*9*) transformed with pmyo5-1 or pMYO5 (*12*). RH3382 and RH3384 were used as controls for strains RH3380 and RH3383 in order to guarantee similar amounts of expression of WT and ts Myo5p. Strains RH3382 and RH3384 behaved in all experiments exactly as did the RH3376 strain, except for α-factor uptake at 37°C, where the initial uptake rates were reduced by approximately 25%.
14. L. Hicke, B. Zanolari, M Pypaert, H. Riezman, in preparation.
15. C. A. McGoldrick, C. Gruver, G. S. May, *J. Cell. Biol.* **128**, 577 (1995).
16. T. S. Stevens, B. Esmon, R. Schekman, *Cell* **30**, 439 (1982).
17. S. Raths, J. Rohrer, F. Crausaz, H. Riezman, *J. Cell Biol.* **120**, 55 (1993).
18. J. Mulholland *et al.*, *ibid.* **125**, 381 (1994).
19. H. Benedetti, S. Raths, F. Crausaz, H. Riezman, *Mol. Biol. Cell* **5**, 1023 (1994); A. L. Munn, B. J. Stevenson, M. I. Geli, H. Riezman, *ibid.* **6**, 721 (1995).
20. *myo2*-66 (10), *tpm1Δ*, *pfy1Δ* (19) strains disrupt the actin cytoskeleton but are not required for endocytosis.
21. C. Lamaze and S. L. Schmid, *Curr. Opin. Cell. Biol.* **7**, 573 (1995); M. Maniak, R. Rauchenberger, R. Albrecht, J. Murphy, G. Gerisch, *Cell* **83**, 915 (1995); K. Sandvig and B. Van Deurs, *J. Biol. Chem.* **265**, 6382 (1990); T. A. Gottlieb, I. E. Ivanov, M. Adesnik, D. D. Sabatini, *J. Cell Biol.* **120**, 695 (1993); G. Jung and J. A. Hammer III, *ibid.* **110**, 1955 (1990).
22. B. Zanolari., S. Raths, B. Singer-Krüger, H. Riezman, *Cell* **71**, 755 (1992).

23. We thank Riezman laboratory members for discussion; S. Schröder, A. L. Munn, A. Wesp, C. Sütterlin, and M. Schönbächler for critical reading of the manuscript; T. Aust and N. Stern for technical assistance; and H. Goodson for the plasmid to delete *MYO3*. Funded by a grant from the Swiss National Science Foundation (to H.R.). M.I.G. was supported by a European Molecular Biology Organization long-term fellowship.

19 December 1995; accepted 12 February 1996

Evaluating Electrostatic Contributions to Binding with the Use of Protein Charge Ladders

Jinming Gao, Mathai Mammen, George M. Whitesides*

Electrostatic interactions between charges on ligands and charges on proteins that are remote from the binding interface can influence the free energy of binding (ΔG_b). The binding affinities between charged ligands and the members of a charge ladder of bovine carbonic anhydrase (CAII) constructed by random acetylation of the amino groups on its surface were measured by affinity capillary electrophoresis (ACE). The values of ΔG_b derived from this analysis correlated approximately linearly with the charge. Opposite charges on the ligand and the members of the charge ladder of CAII were stabilizing; like charges were destabilizing. The combination of ACE and protein charge ladders provides a tool for quantitatively examining the contributions of electrostatics to free energies of molecular recognition in biology.

Although charged groups appear in a majority of biological molecules, and electrostatic interactions between these groups undoubtedly contribute energetically to many important biological interactions, it has been difficult to evaluate these contributions quantitatively. A recent, stimulating review of the influence of electrostatic interactions in biochemistry by Honig (*1*) analyzed this subject in detail and drew a number of startling inferences: for example, in some circumstances (*2*, *3*), interactions between opposite charges may be destabilizing, rather than stabilizing as expected for idealized electrostatic interactions in vacuum (*4*).

Efforts to quantitate electrostatic effects in interactions of proteins with ligands have centered on proteins modified by site-specific mutagenesis (*5*). This technique, although powerful, is labor-intensive and is cumbersome when used to generate proteins that are multiply mutated. Here we summarize the energetics of interaction of the members of a protein charge ladder (*6*) derived from bovine carbonic anhydrase II (CAII) (E.C. 4.2.1.1, containing two isozymes of isoelectric points 5.4 and 5.9, respectively) (*7*) with benzenesulfonamides substituted in the para position with charged and neutral groups. CAII is a roughly spherical Zn(II) metalloenzyme with a conical binding pocket. This pocket is lined with both hydrophobic and polar residues but not with charged residues (*7*). The combination of affinity capillary electrophoresis (ACE) (*8*) and charge ladders derived from CAII and other proteins constitutes a versatile and convenient system with which to define electrostatic contributions to the energetics of the association of charged proteins and charged ligands.

Treatment of CAII with acetic anhydride generates a set of proteins in which distributions of positively charged Lys ε-ammonium groups are converted to neutral *N*-acyl derivatives (Eq. 1).

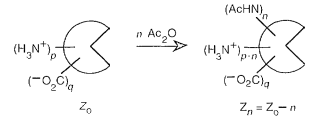

(1)

These sets of modified proteins appear in capillary electrophoresis (CE) as a set of evenly spaced peaks, which we call a "protein charge ladder" (*6*). In Eq. 1, n is the number of acylated amines [CAII has 18 Lys ε-NH_3^+, 26 Asp or Glu-CO_2^-, and 9 Arg-$NHC(NH_2)_2^+$ groups (*7*)], and Z_0 and Z_n are the charges of the native protein and proteins having n modified Lys groups, respectively. In CE, the electrophoretic mobility (μ_n) of a protein is proportional to its charge and inversely correlated with its molecular weight (M)

$$\mu_n \approx \frac{C_P}{M^\alpha} Z_n = \frac{C_P}{M^\alpha} Z_0 - \frac{C_P}{M^\alpha} n \qquad (2)$$

Department of Chemistry, Harvard University, 12 Oxford Street, Cambridge, MA 02138, USA.

*To whom correspondence should be addressed. E-mail: gwhitesides@gmwgroup.harvard.edu